AIChE

Heat Transfer in Nanoparticle Suspensions: Modeling the Thermal Conductivity of Nanofluids

Pramod Warrier, Yanhui Yuan, Michael P. Beck, and Amyn S. Teja
School of Chemical and Biomolecular Engineering, Georgia Institute of Technology, Atlanta, GA 30332

DOI 10.1002/aic.12228
Published online April 5, 2010 in Wiley Online Library (wileyonlinelibrary.com).

This work reviews experimental data and models for the thermal conductivity of nanoparticle suspensions and examines the effect of the properties of the two phases on the effective thermal conductivity of the heterogeneous system. A model is presented for the effective thermal conductivity of nanofluids that takes into account the temperature dependence of the thermal conductivities of the individual phases, as well as the size dependence of the thermal conductivity of the dispersed phase. We demonstrate that this model can be used to calculate the thermal conductivity of nanofluids over a wide range of particle sizes, particle volume fractions, and temperatures. The model can also be used to validate experimental thermal conductivity data for nanofluids containing semiconductor or insulator particles and confirm the size dependence of the thermal conductivity of nanoparticles. © 2010 American Institute of Chemical Engineers *AIChE J,* 56: 3243–3256, 2010
Keywords: nanofluids, nanoparticles, suspensions, phonon scattering, thermal conductivity

Introduction

Interest in sustainable energy has created significant demand for new thermal storage and thermal management technologies, including technologies that employ nanofluids (which are suspensions of nanoparticles in liquids). There is also interest in increasing the efficiency of existing heat transfer processes via improvements in the transport properties of heat transfer media such as nanofluids. The ability to tune the properties of nanofluids offers many advantages in this respect. For example, a 39% increase in the heat transfer coefficient has been reported[1] when an aqueous nanofluid containing 2% (v/v) copper nanoparticles was employed in place of water in forced convective heat transfer experiments in a horizontal tube. Similarly, pool boiling experiments with an aqueous nanofluid containing 1.25% (v/v) alumina nanoparticles have yielded[2] a 40% enhancement in the heat transfer coefficient when compared with the experiments conducted with pure water.

Although heat transfer fluids are generally poor conductors of heat (the thermal conductivity of the most common heat transfer fluid, water, is about 0.6 W m^{-1} K^{-1}), design of more conductive heterogeneous fluids provides an opportunity for improving thermal management efficiency in many applications. The thermal conductivity of a liquid can be increased by the addition of a more thermally conductive liquid or solid. As solid thermal conductivity can be as much as three orders of magnitude greater than that of liquids, research[3,4] has generally focused on liquids containing solid nanoparticles. Many of these studies[3] have reported large increases in the thermal conductivity of the heterogeneous system over that of the base liquid. However, a few studies[5,6] have also produced seemingly conflicting results, particularly with respect to the effect of particle size. A number

Correspondence concerning this article should be addressed to A. S. Teja at amyn.teja@chbe.gatech.edu.

of mechanisms have also been proposed[3,7] to account for the magnitude of the enhancement in the thermal conductivity. These mechanisms have included Brownian motion of particles to create a microconvective effect, the ordering of liquid molecules at the solid interface to enhance conduction, and the clustering of nanoparticles to form pathways of lower thermal resistance. However, models for the thermal conductivity based on one or more of these mechanisms have generally proved ineffective in predicting the thermal conductivity of nanofluids. Thus, fundamental questions remain with respect to the mechanism of thermal conduction in nanofluids as well as the particle size dependence of the thermal conductivity.

This work compiles literature data on the thermal conductivity of nanofluids containing solid semiconductor or insulator particles and critically examines published models for their prediction. On the basis of this evaluation, a model for thermal transport in such nanofluids is proposed and its predictive capabilities are evaluated. The goal is to develop a model that allows the user to tune nanofluid properties, develop new nanofluids, and validate data based on appropriate heat transport mechanisms.

Data Discussion

Thermal conductivity of liquids and solids

As nanofluids are composite materials consisting of a solid discrete phase and a liquid continuous phase, the behavior of their thermal conductivity can best be understood by first considering the behavior of the individual phases. Thermal conductivities of liquids range from about 0.06 W m^{-1} K^{-1} for fluorocarbons to about 0.6 W m^{-1} K^{-1} for water, with nonpolar liquids generally exhibiting lower thermal conductivities than polar liquids. In addition, the thermal conductivity of nonpolar liquids decreases monotonically with increasing temperature due to thermal expansion of the liquid.[8] On the other hand, associating liquids such as water and ethylene glycol display a maximum in their thermal conductivity vs. temperature behavior[9–11] due to changes in the hydrogen bonding network with temperature. At low temperatures, some of the energy being transferred is stored in hydrogen bonds as they form a network, leading to a lower thermal conductivity. As the temperature increases, less energy is captured by the hydrogen bonding network, leading to increased thermal conductivity. This phenomenon competes with the typical decrease in thermal conductivity with temperature due to thermal expansion and results in a maximum in the thermal conductivity—temperature behavior of the fluid.

Heat is conducted in metallic solids by free electrons, and in semiconductors and insulators by lattice waves. As thermal conduction by electrons is more effective than conduction by phonons, the thermal conductivity of metals is generally an order of magnitude greater than that of insulators. The thermal conductivity also depends on the structure of the solid. For example, amorphous carbon has a thermal conductivity of $\sim$1.6 W m^{-1} K^{-1}, but diamond and carbon nanotubes can exhibit[12–14] thermal conductivities as high as 900 and 2000 W m^{-1} K^{-1}, respectively. Crystalline solids typically conduct heat more readily than amorphous solids, and, therefore, their thermal conductivities are higher than those of amorphous solids. In the case of insulators and semiconductors, energy is propagated through the lattice[15] by phonon waves. If the atoms could oscillate harmonically, the velocity of these phonon waves would be the speed of sound in a crystal. However, anharmonicity is observed[16] due to higher order interactions among atoms, and leads to a change in the direction of the phonon wave (or phonon scattering). Phonon scattering can be divided into elastic phonon scattering, where phonon momentum is conserved, and inelastic scattering, where it is not. Inelastic scattering creates resistance to thermal transport and lowers the thermal conductivity. Scattering can result from collisions of phonons with each other (Umklapp scattering) or defects in the crystal structure such as impurities and grain boundaries. Thermal conductivities of semiconductor solids[17] generally increase and then decrease with temperature due to these competing phenomena.

The effect of size of the solid particle on the thermal conductivity has received considerable attention recently. A number of studies[18–20] have focused on thermal conduction in nanoscale semiconductor thin films, and concluded that thermal conductivities of submicron films decrease as the thickness of the film decreases. Indeed, Liu and Asheghi[20] reported that the out-of-plane thermal conductivity of a silicon film of thickness 20 nm was nearly an order of magnitude smaller than the thermal conductivity of bulk silicon. They suggested that phonon scattering at the interface of the solid must become the dominant source of thermal resistance in solid nanomaterials because of their large specific surface area. A less substantial decrease of the in-plane thermal conductivity ($\sim$10% at 300 K) was observed by Yu et al.[21] in a superlattice with a periodic structure of 70 nm.

Phonon–interface scattering is not as well understood as other phonon scattering processes (such as boundary scattering or phonon–phonon scattering), and it is seldom incorporated into models for the thermal conductivity of solids. This could be one reason[22] why most methods are unable to predict the reduced thermal conductivity of nanostructured materials. Ziambaras and Hyldgaard[23] examined the thermal conductivity of nanoscale films and wires using the Boltzmann transport equation with phonon–interface scattering and found that the axial thermal conductivity of a wire is less than the in-plane thermal conductivity of a film of the same thickness. They suggested that this effect is similar to Knudsen diffusion, and is caused by confinement of the phonon wave when the phonon mean free path is of the same order as the thickness of the nanomaterial. Nanowires, which are confined in two dimensions, are therefore expected to exhibit a lower thermal conductivity than nanofilms, which are only confined in one dimension. Li et al.[24] demonstrated this phenomenon when they measured axial heat conduction in silicon nanowires. They reported that the axial thermal conductivity of a 22 nm diameter silicon nanowire was approximately 6 W m^{-1} K^{-1}, while the out-of-plane thermal conductivity for a 20-nm-thick silicon film was about 22 W m^{-1} K^{-1}. The nanowire value is more than two orders of magnitude lower than the bulk thermal conductivity of silicon (237 W m^{-1} K^{-1}).

Semiconductor nanoparticles should exhibit an even lower thermal conductivity than nanowires or nanofilms, because

nanoparticles are confined in three dimensions. Fang et al.[25] used molecular dynamic simulations to estimate the thermal conductivity of silicon nanoparticles and reported that the thermal conductivity of particles smaller than 8 nm was about 2 W m^{-1} K^{-1}. In contrast, the thermal conductivity of bulk silicon is 237 W m^{-1} K^{-1} as noted previously. These results have yet to be confirmed experimentally, although it seems clear that the thermal conductivity of semiconductor or insulator particles must decrease with particle size when the particle size approaches the mean free path of phonons in the solid.

The studies described above imply that the contribution of the particle thermal conductivity to the effective thermal conductivity of a solid dispersion should also decrease as the size of the dispersed particles approaches the phonon mean free path. The following sections review data and models related to the thermal conductivity of dispersions of solid particles in liquids.

Thermal conductivity of micro and nanoparticle dispersions

Although there have been numerous studies related to the transport properties of microparticle suspensions, only two are mentioned here because their conclusions relate directly to the behavior of nanoparticle suspensions. Shin and Lee[26] reported that the effective thermal conductivity of 10% (v/v) dispersions of micron-sized polyethylene and polypropylene particles in mixtures of silicon oil and kerosene was about 13% greater than the thermal conductivity of the base fluid. Moreover, they found a linear relationship between the effective thermal conductivity of the heterogeneous system and the volume fraction of particles. Turian et al.[27] measured the thermal conductivity of a number of fluids containing as much as 50% (v/v) of dispersed coal, glass, gypsum, or silica particles and reported modest increases in the thermal conductivity. For example, they observed an 18% increase in the thermal conductivity in an aqueous dispersion containing 12% (v/v) silica particles. In addition, a linear relationship between the thermal conductivity and particle volume fraction was observed, although there was a change in slope at about 0.1 volume fraction.

Fluids containing dispersed nanoparticles have been extensively studied since Choi[28] reported that heat transfer in liquids could be considerably enhanced by the addition of metallic nanoparticles. Thus, Eastman et al.[29] found that the addition of 0.3% (v/v) copper nanoparticles to ethylene glycol resulted in an increase of 40% in the thermal conductivity of the liquid, although about 1% (v/v) thioglycolic acid was also added to the liquid to aid in dispersing the nanoparticles. Jana et al.[30] measured the thermal conductivity of a similar nanofluid, except that the base fluid was water containing laurate salt as a dispersant. They obtained a 70% thermal conductivity enhancement when 0.3% (v/v) copper nanoparticles were added to water. These large enhancements were attributed to increased transport resulting from the large surface area of the particles. Equally large thermal conductivity enhancements have been reported when metal oxides are added to liquids. An early study by Eastman et al.[31] reported that an aqueous nanofluid containing 5% (v/v) copper oxide nanoparticles exhibited a thermal conductivity that was 60% greater than that of water, and another aqueous nanofluid containing 5% (v/v) alumina nanoparticles exhibited a thermal conductivity that was 40% greater than that of water. More recent studies, however, have reported more modest enhancements[32–35] in similar nanofluids. It should also be added here that differences in reported values of the enhancement are quite common in the nanofluid literature. On the other hand, extremely large enhancements have been reported when carbon nanotubes are dispersed in liquids. According to Yang et al.,[36] the addition of 0.35% (v/v) of multiwalled carbon nanotubes (MWCNT) to poly (α-olefin) oil results in a 200% thermal conductivity enhancement; whereas, Choi et al.[14] have stated that a 150% thermal conductivity enhancement is obtained when 1% (v/v) MWCNT are added to poly(α-olefin) oil. It is clear from these studies that there is a significant increase in the thermal conductivity when solid particles are added to liquids, although the magnitude of the enhancement is not yet established. The enhancement is, however, proportional to the thermal conductivity of the dispersed particles.

Effect of volume fraction

Most studies of nanofluids have reported a linear relationship between the effective thermal conductivity and volume fraction of particles (as shown in Figure 1), although a few studies[41,42] have also reported a change in slope when volume fractions are very small. The magnitudes of the reported enhancements in dilute systems have ranged from unusually high[29,30,43,44] to negligibly small.[34,45]

Effect of particle size

The particle-size dependence of the thermal conductivity of dispersions has received considerable attention because of

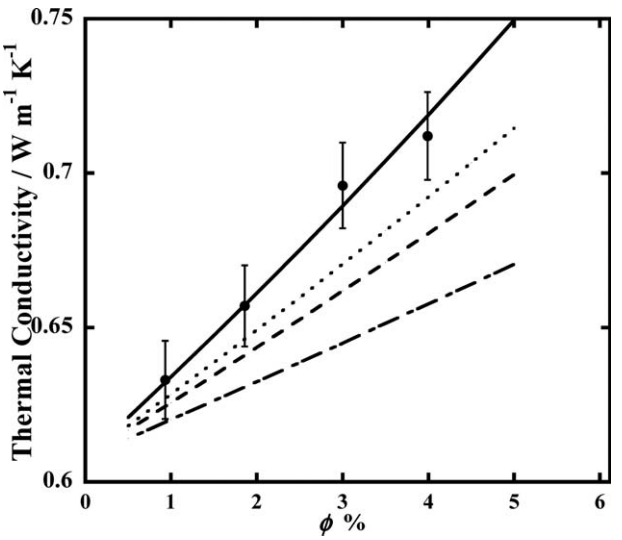

Figure 1. Thermal conductivity of an aqueous nanofluid containing 71 nm diameter alumina particles as a function of volume fraction ϕ.

Data of Beck et al.[37] (●). Error bars represent the estimated measurement error. Lines represent predictions of the Maxwell[38] (– –), Nan et al.[39] (— - —), Yu and Choi[40] (…), Geometric mean[27] (—) models.

the widely held view that increasing surface to volume ratios must lead to enhanced heat transfer (and hence higher thermal conductivity) as the particle size decreases. Thus, Kim et al.[6] reported that enhancements obtained when 10 nm titania particles are dispersed in ethylene glycol are about twice those obtained when 70 nm particles are dispersed in the same fluid at the same volume fraction. Li and Peterson[46] also reported that enhancements in aqueous alumina nanofluids were 8% higher for 36 nm particles than for 47 nm particles. On the other hand, Xie et al.[5] reported that the thermal conductivity enhancement in alumina nanofluids exhibits a maximum at particle sizes between 12 and 304 nm. More recently, Beck et al.[37,47] reported that the thermal conductivity of alumina nanofluids decreases with particle size below about 50 nm. This behavior is consistent with a decrease in the thermal conductivity of alumina particles with decreasing particle size.

Effect of temperature

Das et al.[48] measured the thermal conductivity of aluminum and copper oxide nanofluids in water at temperatures between 293 and 323 K and concluded that the thermal conductivity of nanofluids increases with temperature. In contrast, Yang and Han[49] studied dispersions of Bi_2Te_3 nanorods in perfluorohexane and reported a decrease in the effective thermal conductivity as the temperature increased from 278 to 323 K. As noted previously, the thermal conductivity of nonpolar liquids generally decreases monotonically with increasing temperature,[8] whereas that of associating liquids such as water generally exhibits a maximum in the thermal conductivity vs. temperature behavior.[9,10] In the case of water, the maximum occurs at ~404 K. As many of the measurements on aqueous nanofluids have been made at temperatures below 400 K, they are in the region where the thermal conductivity of water increases with temperature. Also, as the volume fraction of particles in nanofluids is generally small, it is likely that the thermal conductivity of nanofluids is dominated by the thermal conductivity of the base fluid. To confirm this hypothesis, Beck et al.[50] measured the thermal conductivity of ethylene glycol–based alumina nanofluids at temperature ranging from 298 to 411 K and found that the thermal conductivity vs. temperature behavior of the nanofluid follows closely that of the base fluid (ethylene glycol in this case). This behavior is shown in Figure 2 and has also been validated[47] when the base fluid is water or a mixture of water and ethylene glycol.

Effect of the particle to fluid thermal conductivity ratio α

Xie et al.[51] measured the thermal conductivity of 60 nm alumina particles dispersed in different base fluids, and found larger enhancements when values of α ($= k_p/k_l$) were large. For example, the enhancement for alumina in pump oil ($\alpha = 326$) was about 40%, whereas that for alumina in water ($\alpha = 75$) was about 23%. Similar trends have been noted[48,52–55] in nanofluids with the same base fluid but containing different nanoparticles. Also, some of the largest thermal conductivity enhancements have been observed in nanofluids containing highly thermally conductive particles (such as copper,[29] carbon nanotubes,[14] and diamond[13]).

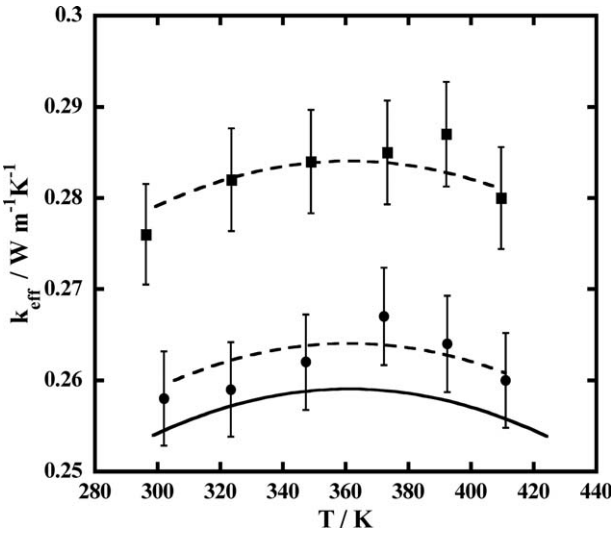

Figure 2. Thermal conductivity–temperature behavior of alumina nanofluids in ethylene glycol.

Data of Beck et al.[50] at particle concentrations of 1 % (v/v) (●) and 3% (v/v) (■). The solid line represents literature data for ethylene glycol, whereas dashed lines represent fits of the nanofluid data.

Effect of particle surface charge

Lee et al.[56] varied the pH of the solution before dispersing nanoparticles and observed greater thermal conductivity enhancement in acidic and basic solutions, and a lower enhancement at neutral pH values. They concluded that surface charges increase the stability of the dispersion leading to an increased thermal conductivity.

Effect of particle arrangement in suspension

Wright et al.[57] studied the thermal conductivity of dilute nanofluids containing 0.01–0.02% Nickel-coated single-walled carbon nanotubes (SWCNT) within a magnetic field. They observed greater thermal conductivity enhancement when the magnetic field was applied, which suggests that the nanotubes aligned to form conductive paths within the fluid. Hong et al.[58] and Wensel et al.[59] observed similar behavior in dilute nanofluids containing both iron oxide and SWCNTs. However, the thermal conductivity decreased after some time in the magnetic field due to agglomeration and settling of particles.

Summary of Findings

The following trends may be discerned from the studies outlined in the preceding paragraphs:

(i) The addition of solid particles to liquids generally leads to a change in the effective thermal conductivity of nanofluids, in proportion to the amount (volume fraction) of particles added, and to the thermal conductivity of the solid particles.

(ii) Thermal conductivity enhancements in the case of dilute nanofluids containing dispersed semiconductor or insulator particles are generally less than 25%, although a few studies have reported much larger enhancements.

(iii) The temperature dependence of the effective thermal conductivity of nanofluids conforms closely to that of the base fluid.

(iv) The effective thermal conductivity decreases with decreasing size of dispersed particles, when particles are very small.

(v) The stability of the suspension and particle aggregation affects the thermal conductivity of nanofluids, although the magnitude of these effects has not been determined quantitatively.

The following paragraphs describe models for the effective thermal conductivity of dispersions and examine their applicability in light of these trends.

Model Evaluation

Models for microparticle dispersions

Maxwell[38] derived the following relationship for the thermal conductivity of dilute suspensions of spherical particles:

$$\frac{k_{\text{eff}}}{k_{\text{l}}} = 1 + \frac{3(\alpha - 1)\phi}{(\alpha + 2) - (\alpha - 1)\phi} \tag{1}$$

where k_{eff} is the effective thermal conductivity of the dispersion, α is the ratio $(k_{\text{p}}/k_{\text{l}})$ of thermal conductivity of the particle to that of the fluid, and ϕ is the particle volume fraction. The model is applicable to uniform dispersions of spherical particles when there are no particle interactions. Rayleigh[60] extended the Maxwell model to concentrated dispersions by considering spheres or cylinders arranged in a cubic lattice, whereas Hamilton and Crosser[61] proposed an extension that included an empirical factor n to account for the shape of particles as follows:

$$\frac{k_{\text{eff}}}{k_{\text{l}}} = 1 + \frac{n(\alpha - 1)\phi}{(\alpha + n - 1) - (\alpha - 1)\phi} \tag{2}$$

In Eq. 2, $n = 3/\psi$ and ψ is the sphericity of the particle. A second order extension of the Maxwell model was proposed by Jeffrey[62] by considering the effect of interactions between pairs of spheres. Models based on the effective medium theory were proposed by Progelhof et al.[63] and Landauer.[64]

Maxwell type models generally imply an effective thermal conductivity that increases with the volume fraction of particles, is dependent mostly on the thermal conductivity of the base liquid, and is 0–15% greater than that of the base liquid when $\phi < 0.05$. Turian et al.[27] demonstrated that these models, including those proposed by Maxwell,[38] Jeffrey,[62] and Progelhof et al.[63] are able to fit experimental data for dilute suspensions within 2% when $0.4 < \alpha < 2.4$. Agreement with experiment becomes less satisfactory as α increases and also as ϕ increases. Note that increasing ϕ often leads to particle aggregation and this cannot be accounted for by these models.

Krischer[65] considered an array of elements of specific resistance distributed in a matrix, and obtained:

$$k_{\text{eff}} = \left[\frac{1 - f}{(1 - \phi)k_{\text{l}} + \phi k_{\text{P}}} + f\left(\frac{1 - \phi}{k_{\text{l}}} + \frac{\phi}{k_{\text{P}}}\right)\right]^{-1} \tag{3}$$

where f is an empirical factor equivalent to the fraction of parallel resistances in a rectangular array of elements. This model can be used to determine upper and lower bounds for the thermal conductivity of a heterogeneous system, with $f = 0$ signifying that all particles are arranged in series (creating a high thermal conductivity pathway) and $f = 1$ signifying that all particles are arranged in parallel (creating a low thermal conductivity arrangement). The actual value of f must be obtained by experiment. Tsao[66] developed a similar model by considering different geometries of the discrete phase, whereas Hashin and Shtrikman[67] derived more restrictive bounds using the variational theorem. Their bounds may be expressed as:

$$1 + \frac{3\phi(\alpha - 1)}{\alpha + 2 - \phi(\alpha - 1)} \leq \frac{k_{\text{eff}}}{k_{\text{l}}} \leq \alpha\left[1 - \frac{3(\alpha - 1)(1 - \varphi)}{3\alpha - \phi(\alpha - 1)}\right] \tag{4}$$

In Eq. 4, the lower bound is the Maxwell limit. The upper bound implies an effective thermal conductivity that is higher than the Maxwell limit when particle aggregation is significant.

Turian et al.[27] noted that the upper and lower bounds of the Krischer model are equal to the volume-fraction-weighted arithmetic and harmonic means of the thermal conductivities of the two phases. The geometric mean of the two thermal conductivities falls between these bounds and also falls within the more restrictive Hashin–Shtrikman bounds when $\alpha > 5$. Therefore, Turian et al. used the volume-fraction-weighted geometric mean of the thermal conductivities of the individual phases defined by:

$$\frac{k_{\text{eff}}}{k_{\text{l}}} = \alpha^{\phi} \tag{5}$$

to calculate thermal conductivities of their suspensions. They found that the Maxwell model was able to fit data within 14.3%, whereas Eq. 5 could predict data within 5.7% of experimental values when $3.5 < \alpha < 70$. When $70 < \alpha < 200$, the average deviation was 26.3% for the Maxwell equation and 9.9% for Eq. 5. Turian et al. concluded that Eq. 5 provides good estimates of the effective thermal conductivity for particle suspensions when $\alpha > 3.5$. It should be added here that particle sizes in their suspensions were relatively large (of the order of microns).

Similar "mixture models" for the effective thermal conductivity of composites have also been proposed.[68,69] These models may be summarized as follows:

$$(k_{\text{eff}})^n = \phi(k_{\text{p}})^n + (1 - \phi)(k_{\text{l}})^n \qquad -1 < n < 1 \tag{6}$$

When $n = 1$, Eq. 6 reduces to the arithmetic mean of the thermal conductivities of the two materials, and provides a good representation for conduction in materials arranged in parallel. Similarly, when $n = -1$, Eq. 6 reduces to the harmonic mean of the two thermal conductivities, and provides

a representation for conduction in materials arranged in series. Finally, for n approaching zero, Eq. 6 reduces to the geometric mean of the thermal conductivities of the two materials. As discussed previously, Turian et al.[27] have shown that the geometric mean works well in heterogeneous suspensions of micron-sized particles. Their conclusions agree with those of Prasher et al.[70] who suggested further that particle aggregation would result in thermal conductivity enhancements that are greater than those predicted by the Maxwell equation. None of these models, however, include any particle size dependence.

Nanofluid models

Several mechanistic models for heat transport in nanofluids have been proposed to account for thermal conductivities that exceed values predicted by the Maxwell equation. These models are discussed below.

Yu and Choi[40] proposed a contribution to the thermal conductivity of nanofluids from an ordered liquid layer at the solid–liquid interface. This ordered layer is assumed to have a higher thermal conductivity than the bulk liquid, leading to an effective thermal conductivity given by:

$$\frac{k_{\text{eff}}}{k_{\text{l}}} = \frac{k_{\text{pe}} + 2k_{\text{l}} + 2(1+\beta_{\text{l}})^3(k_{\text{pe}} - k_{\text{l}})\phi}{k_{\text{pe}} + 2k_{\text{l}} - (1+\beta_{\text{l}})^3(k_{\text{pe}} - k_{\text{l}})\phi} \tag{7}$$

where β_{l} is the ratio of the ordered liquid layer thickness to the nanoparticle radius, and k_{pe} is the effective thermal conductivity of the particle defined by:

$$k_{\text{pe}} = \frac{\left[2(1-\gamma) + (1+\beta_l)^3(1+2\gamma)\right]\gamma}{(1+\beta_l)^3(1+2\gamma) - (1-\gamma)} k_p \tag{8}$$

Here, γ is the ratio of the thermal conductivity of the ordered liquid layer to that of the solid particle. Similar models based on an effective particle size that includes the surrounding ordered liquid layer have been proposed by others.[71–76] These models imply an inverse relationship of the effective thermal conductivity with particle size, and generally treat the thickness and thermal conductivity of the ordered liquid layer as adjustable parameters. However, values of the ordered layer thickness obtained by fitting data were found[73] to be between 1 and 3 nm, and the thermal conductivity of the ordered layer was reported[40,74] to be about 5–10 times the thermal conductivity of the base fluid. In contrast, Li et al.[77] and Evans et al.[78] used MD simulations to estimate an ordered layer thickness of about 0.5 nm, and an ordered layer thermal conductivity of crystalline water to be about three times that of liquid water. Neither of these values is in agreement with that obtained by fitting data. Moreover, use of values from MD simulations leads to enhancements that are about the same as those predicted by the Maxwell equation, except when particle diameters are less than 5 nm.

A number of models attribute the enhanced thermal conductivity of nanofluids to a local microscale convective effect created by Brownian motion of particles. As an example, the Jang and Choi[79] equation combines contributions from the liquid, suspended particles, and Brownian motion of the particles to obtain:

$$\frac{k_{\text{eff}}}{k_{\text{l}}} = (1-\phi) + \varepsilon\alpha\phi + \phi C_1 \frac{d_{\text{f}}}{d} \text{Re}^2 \,\text{Pr} \tag{9}$$

where ε is a constant related to the interfacial thermal resistance, C_1 is a proportionality constant, d_{f} is the diameter of a fluid molecule, d is the particle diameter, and Re and Pr are the Reynolds and Prandtl numbers, respectively, based on the properties of the fluid. However, it has been demonstrated[27] that a linear combination of the individual thermal conductivity contributions is a poor predictor of the effective thermal conductivity of heterogeneous systems. This has led some researchers[80–84] to incorporate Brownian motion based particle size dependence directly into conventional thermal conductivity models for heterogeneous systems. For instance, Xuan et al.[83] included the microconvective effect of the dynamic particles in the Maxwell equation to obtain:

$$\frac{k_{\text{eff}}}{k_{\text{l}}} = \frac{\alpha + 2 + 2\phi(\alpha - 1)}{\alpha + 2 - \phi(\alpha - 1)} + \frac{18\phi H A\, k\, T}{\pi^2 \rho d^6 k_{\text{l}}} \tau \tag{10}$$

where H is the overall heat transfer coefficient between the particle and the fluid, A is the corresponding heat transfer area, and τ is a comprehensive relaxation time constant. The heat transfer area is proportional to the square of the diameter, leading to an effective thermal conductivity that is inversely proportional to the fourth power of the particle diameter. Such strong inverse dependence on particle size has not been demonstrated experimentally. In addition, Eq. 10 reduces to the Maxwell equation with increasing particle size, and cannot, therefore, account for thermal conductivities that are greater than the Maxwell limit.

Models that incorporate an interfacial thermal resistance into the Maxwell equation have been published by Nan et al.[39] and others. The interfacial thermal resistance is related to the different rates of transport in the two phases that lead to a temperature discontinuity at the solid–liquid interface. The interfacial resistance is sometimes referred to as the Kapitza resistance[85] and includes the effects of phonon scattering at the interface, as well as other phenomena that create resistance to heat transport such as poor contact between the phases. For spheres, the Nan et al. model can be written as follows:

$$\frac{k_{\text{eff}}}{k_{\text{l}}} = \frac{\alpha(1+2\chi) + 2 + 2\phi[\alpha(1-\chi) - 1]}{\alpha(1+2\chi) + 2 - \phi[\alpha(1-\chi) - 1]} \tag{11}$$

where $\chi = 2R_{\text{B}}k_{\text{l}}/d$ and R_{B} is the interfacial thermal resistance. Eq. 11 reduces to the Maxwell equation when $\chi \ll 1$ and is thus incapable of representing enhancements that are greater than those predicted by the Maxwell equation. However, it correctly predicts a decrease in effective thermal conductivity with particle size.

Another type of model takes account of particle aggregation in nanofluids and was proposed by Prasher et al.[70] Their model assumes that particle aggregates form conductive pathways in the fluid resulting in enhancements that are greater than those predicted by the Maxwell model. However, the model requires information on aggregate size as

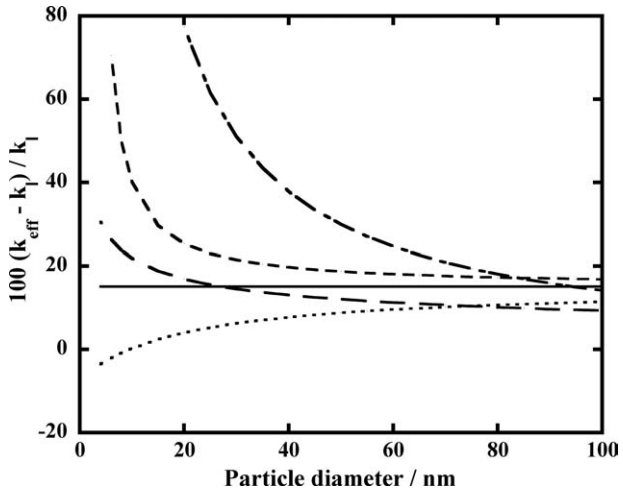

Figure 3. Calculated thermal conductivity enhancement as a function of particle size for an aqueous nanofluid containing 5% (v/v) alumina at room temperature from several models.

Maxwell[38] —, Nan et al.[39] …, Yu and Choi[40] – – , Chon et al.[89] — —, and Jang and Choi[79] — - —.

well as the fraction of particles forming conductive pathways. These quantities are seldom available, although the hypothesis that particle clustering enhances conduction in suspensions is supported by numerical simulations and molecular dynamics studies.[86–88]

Figure 3 displays a comparison of thermal conductivity predictions from various models and their relationship with particle diameter. With the exception of the Nan et al. model, all models described above predict an inverse relationship between nanofluid thermal conductivity and particle size. The models therefore predict an increase in the effective thermal conductivity as the particle size decreases. As noted previously, the thermal conductivity of thin films and nanowires decreases with decreasing size[23] and this trend should be more pronounced in nanoparticles due to confinement of phonon waves in all three dimensions. Recent experimental data[37,47,90] confirm such a trend. Thus, none of the above models are able to correctly predict both the size dependence of the effective thermal conductivity and enhancements that are greater than the Maxwell limit.

Modified Geometric Mean Model

All published models for the thermal conductivity of nanofluids predict a linear dependence of the enhancement on particle volume fraction, which is confirmed by published data. However, as shown in Figure 1, the magnitude of the thermal conductivity is not necessarily predicted well by all models. In addition, the dependence with respect to temperature and particle size is not represented adequately by many of these models. The Nan et al.[39] model reproduces the general trends of thermal conductivity data with particle volume fraction, temperature, and particle diameter. However, the model reduces to the Maxwell model at large particle sizes and cannot, therefore, reproduce enhancements that are greater than those predicted by the Maxwell model.

Figure 4 compares predictions of the geometric mean and Maxwell models with experimental data on nanofluids containing alumina particles larger than 50 nm. The predictions of the geometric mean model are within 2% of experimental values irrespective of the base fluid (pump oil, ethylene glycol, glycerol, or water). It would, therefore, appear that the geometric mean is capable of predicting the limiting value of the thermal conductivity of alumina nanofluids. However, the geometric mean model does not explicitly include any particle size dependence.

Liang and Li[91] recently proposed a phenomenological theory for the size dependence of the thermal conductivity of semiconductors and insulators by taking into account the intrinsic size effect on phonon velocity, mean free path, and surface scattering. An advantage of their model is that the same equation can be used for thin films, nanowires, and nanoparticles. According to Liang and Li,[91] the thermal conductivity of a nanostructure is given by:

$$\frac{k_p(L)}{k_b} = p\exp\left(-\frac{l_0}{L}\right)\left[\exp\left(\frac{1-A}{L/L_0-1}\right)\right]^{3/2} \tag{12}$$

where $k_p(L)$ is the thermal conductivity of the nanostructure of characteristic size L, k_b is the thermal conductivity of the bulk material, l_0 is the phonon mean free path at room temperature, and L_0 is the critical size when almost all atoms of the crystal are located on its surface. L_0 may be obtained from:

$$L_0 = 2(3-n)\sigma \tag{13}$$

where σ is the atomic/molecular diameter, and $n = 0$, 1, and 2 for nanoparticles, nanowires, and thin films, respectively. Parameter A depends on the bulk vibrational entropy of melting S_v as follows:

$$A = 1 + (2/3)S_v/R \tag{14}$$

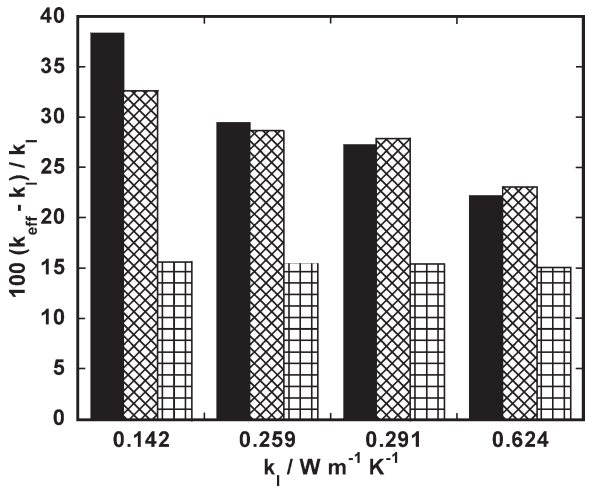

Figure 4. The thermal conductivity of 5% (v/v) alumina in pump oil, ethylene glycol, glycerol, and water.

Data of Xie et al.[51] (■) and predictions of Maxwell[38] (▦) and geometric mean[27] (▨) models.

Table 1. Characteristic Constants for Eqs. 12–16

	k_b (W m^{-1} K^{-1})	$\rho \times 10^3$ (kg m^{-3})	C_p (J mol^{-1} K^{-1})	v_a (m s^{-1})	l_0 (nm)	H_m (kJ mol^{-1})	T_m (K)	σ (nm)
Si	236.8[25]	2.33[93]	19.99[94]	6351[95]	41[91]	50.55[91]	1685[91]	0.2352
α-Al_2O_3	40[93]	3.97[96]	78.96[96]	6763	5.77	55.12[94]	2345[96]	0.238
TiO_2 (Rutile)	8.4[6]	4.23[96]	54.76[96]	5568	1.56	44.67[96]	2116[96]	0.1475
CeO_2	10.4[93]	7.65[96]	61.53[96]	6052	2.18	87.18[93]	2673[96]	0.3825
CuO	77[97]	6.31[96]	42.26[96]	5000*	13.78	11.79[93]	1719[96]	0.195
Fe_3O_4	7[98]	5.17[96]	143.37[96]	2500[98]	2.56	137.94[93]	1870[96]	0.5954
SiO_2	1.34[99]	2.65[96]	44.57[94]	3863	0.58	8.78[93]	1996[96]	0.245
ZnO	29[6]	5.61[96]	40.21[96]	3159	9.94	18.69[93]	2248[96]	0.1625
α-SiC	490[99]	3.22[95]	26.74[97]	7893[93]	86.73	3.18[120]	2973[96]	0.1535
Diamond	900[100]	3.51[95]	6.57[94]	13826[95]	104.81	104.6[101]	4093[101]	0.1546

*assumed value.

where R is the universal gas constant. For III–V and II–VI compounds, $S_v = H_m/T_m - R$, where H_m is the enthalpy of melting and T_m is the bulk melting point. For molecular crystals,[92] $S_v = S_m = H_m/T_m$. The adjustable parameter p ($0 < p \leq 1$) in Eq. 12 provides a measure of surface roughness and is discussed further below.

Liang and Li[91] successfully tested Eq. 12 for thin films and nanowires but could not validate the equation for nanoparticles because of lack of experimental data. In our work, we have used Eqs. 12–14 and the physical parameters given in Table 1 to calculate the thermal conductivity of nanoparticles. The phonon mean free path l_0 was calculated using the kinetic theory expression:

$$k = \frac{1}{3}\rho\, C_v v_a l_o \tag{15}$$

where ρ is the density, C_v is the specific heat, and v_a is the average phonon velocity. Bulk values of the properties of the material at 300 K were used to obtain l_o. The average phonon velocity v_a was calculated using[17]:

$$\frac{3}{v_a^3} = \frac{1}{v_l^3} + \frac{2}{v_t^3} \tag{16}$$

where v_l is the velocity of the longitudinal wave and v_t is the velocity of the (two) transverse waves in the material of interest. Crystal structure and lattice constants were obtained from Bragg et al.[102] and Yang et al.[119] For molecular crystals, σ was calculated from nearest-neighbor separation of molecules in the molecular lattice.[103] Jiang et al.[104] pointed out that the entropy of melting is not sensitive to σ, especially when L/σ is large ($L > 4$ nm, and $\sigma < 0.5$ nm). Table 2 compares calculated phonon mean free paths for several oxides with published values and confirms that the kinetic theory expression provides reasonable estimates of l_o. Calculated thermal conductivity of several semiconductors and insulators are plotted in Figure 5. It can be seen that the effective thermal conductivity of these materials attains its bulk value at particle sizes of about 100 nm.

Table 2. Calculated Phonon Mean Free Path l_0/nm at 298 K for Several Semiconductors

	Literature Value	Eq. 15
Al_2O_3	5.08[105]	5.77
SiO_2	0.6[105]	0.58
SiC	69.05[106]	86.73

The size-dependent thermal conductivity from Eq. 12 was incorporated into the volume fraction weighted geometric mean to obtain a modified geometric mean model as follows:

$$\frac{k_{eff}}{k_l} = \left[\frac{k_p(L)}{k_l}\right]^{\phi} \tag{17}$$

where $k_p(L)$ is the thermal conductivity of the nanoparticle from Eq. 12. Figure 6 compares the fits of Eq. 5 (geometric mean model) and Eq. 17 (modified geometric mean model) to experimental data for alumina nanofluids.[37,47] Eq. 17 was fitted by minimizing the average absolute deviation in k_{eff} with p as the adjustable parameter. Optimized values for each particle size are as follows: 8 nm, $p = 0.12$; 12 nm, $p = 0.21$; 16 nm, $p = 0.28$; 71, 245, and 282 nm, $p = 1$. To ascertain if the values of p obtained are physically realistic, the relation[91] $p = 1 - 10\,\eta/L$ was used to calculate the surface roughness η. The surface roughness was found to be less than 10% of the particle size in all cases, which appears to be reasonable.

Figure 7 shows predictions of the thermal conductivity of alumina nanofluids in water and ethylene glycol using Eq. 17. A single value of p was used for each particle size irrespective of the base fluid or temperature. For example, for 12 nm alumina particles, a value of $p = 0.28$ was

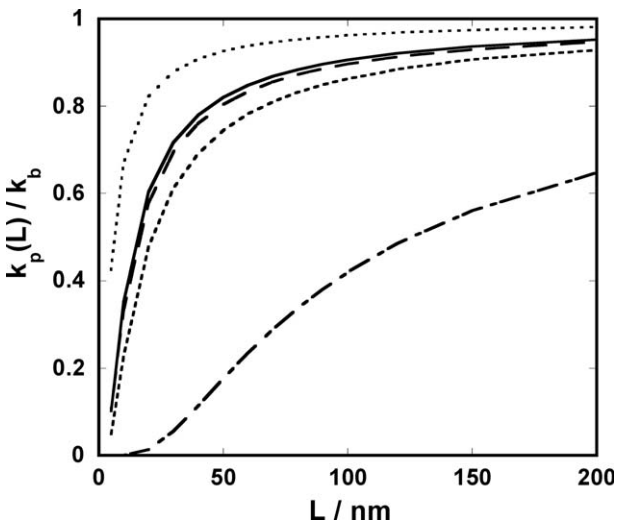

Figure 5. Thermal conductivity of semiconductors and insulators calculated using Eq. 12. Al_2O_3 (—), TiO_2 (. . .), CuO (– –), ZnO (— —), SiC (— - —).

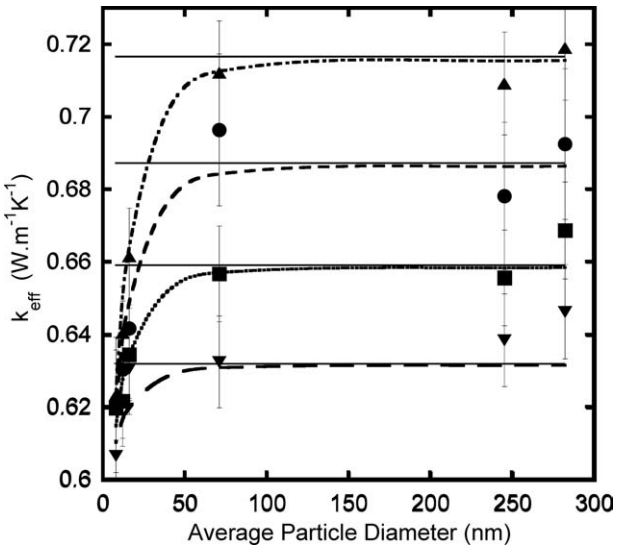

Figure 6. Thermal conductivity enhancement in aqueous nanofluids containing 1–4% (v/v) alumina particles at room temperature.

Points (1% ▼, 2% ■, 3% ●, 4% ▲) represent experimental values of Beck et al.,[37] lines represent calculations using Eq. 5 (solid line) and Eq. 17 (dashed lines).

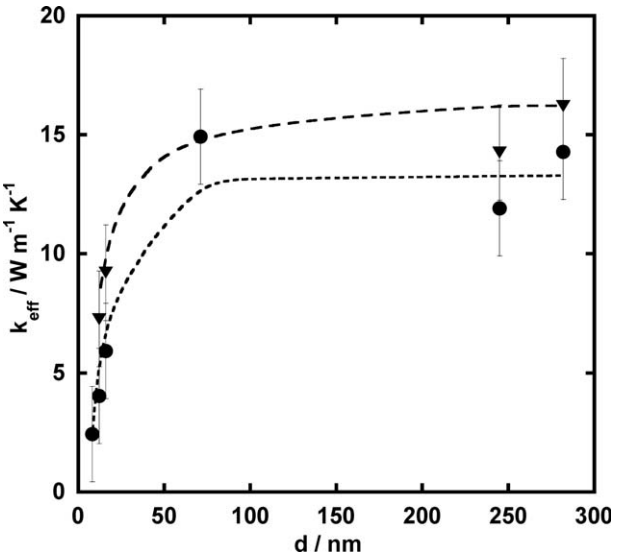

Figure 7. Thermal conductivity enhancement in water- (●) and ethylene glycol- (▼) based nanofluids containing 3% (v/v) alumina particles at 298 K as a function of particle size.

Dashed lines (water - - - -, EG – –) represent Eq. 17 using the same values of p as in Figure 6.

obtained by fitting the nanofluid data of 12 nm alumina particles in water as well as in ethylene glycol. It is clear that Eq. 17 is able to account for the decrease in thermal conductivity with decreasing particle size in the two base fluids. Thus, when surface roughness must be taken into account, the parameter p can be obtained by fitting data for one base fluid. The same value of p may then be used to predict the thermal conductivity behavior in a different base fluid.

Tables 3–11 list average deviations between experimental thermal conductivities of several nanofluids and calculated values using Eqs. 5 and 17. In the case of alumina nanofluids, comparisons are also shown with the Nan et al model (Eq. 11). Because of lack of published data on interfacial thermal resistance, the Nan et al model could not be evaluated for other nanofluids. Optimized values of p were therefore obtained for alumina nanofluids only and are given in Table 3. Thermal conductivities of the base fluids were obtained by fitting literature data[10,11] as follows: k_{H2O} = 1.8822 E-8 T^3 − 2.7872 E-5 T^2 + 0.013274 T − 1.371; k_{EG} = 0.088067 + 9.4712 E-4 T − 1.3114 E-6 T^2. Thermal conductivities of the solids were assumed to be independent of

Table 3. Comparing the Geometric Mean (GM), Modified Geometric Mean (mGM), and Nan et al. Models with Experimental Data for Alumina Nanofluds

				Average Absolute Deviation (%)			
Data Reference	Particle Size (nm)	Fluid	T (K)	Nan et al. Model[39]	GM	mGM	mGM (p)
31	33	Water	298	11.03	3.2	3.87	3.87 (1)
107	35	Water	298	5.46	2.76	2.09	0.47 (0.54)
54	38.4	Water	298	2.28	5.55	4.98	0.19 (0.18)
	38.4	EG	298	3.81	5.64	5.04	0.58 (0.18)
53	28	Water	298	8.17	4.71	3.39	2.52 (0.75)
	28	EG	298	15.8	3.74	2.68	2.36 (0.75)
5,51	60.4	Water	298	8.79	1.32	1.56	1.56 (1)
	12.4–302	EG	298	7.29	4.39	3.39	1.48 (0. 3)
48	38.4	Water	294–324	6.88	3.61	3.56	3.52 (0.86)
89	13–182	Water	294–344	6.69	4.36	4.46	4.46 (1)
52	36	Water	301–309	7.97	13.54	12.53	6.47 (0.14)
32–34	20	Water	283–323	5.74	20.32	16.48	2.14 (0.09)
6	38	Water	298	1.57	2.09	1.83	0.16 (0.24)
	38	EG	298	2.85	3.42	3.02	0.15 (0.24)
46	36 and 47	Water	302–310	5.19	4.11	3.89	3.48 (0.54)
35	11–40	Water	296–333	4.59	14.89	12.13	1.93 (0.13)
	11–40	EG	296–333	4.06	15.43	12.98	2.11 (0.13)
108,109	48	Water	298	2.53	0.61	0.71	0.71 (1)
110	45	Water	298	1.76	4.62	1.45	0.69 (0.63)
	45	EG	298	7.38	1.04	6.97	5.75 (0.63)

Average absolute deviation (%) for n data points = Σ abs $(k_{exp} - k_{pred})/k_{exp} \times 100/n$.

Table 4. Comparing the Geometric Mean (GM) and Modified Geometric Mean (mGM) Models with Experimental Data for Titania Nanofluids

				Average Absolute Deviation (%)	
Data Reference	Particle Size (nm)	Fluid	Temperature (K)	GM	mGM (p)
41	15	Water	298	11.02	11.55 (1)
6	10–79	Water	298	1.16	1.46 (1)
	10–79	EG	298	1.76	2.05 (1)
109	25	Water	298	9.54	9.62 (1)
111	26	Water	291–338	0.78	0.76 (1)
32	40	Water	283–313	0.66	0.49 (0.93)
118	2	Water + EG	297–421	33.12	2.99 (0.07)
112	21	Water	288–308	1.13	1.09 (0.92)

temperature within the temperature ranges encountered in this study.

Tables 3–11 show that deviations between experimental and predicted thermal conductivities using the modified geometric mean model are generally less than ±3%. Deviations greater than ±3% occur when the reported experimental value is unusually high, or when the effect of particle size or temperature is not in agreement with the experimental trends noted above. For example, Li[52] reported a linear increase in thermal conductivity with temperature for alumina nanofluids and also ignored the temperature dependence of the thermal conductivity of their base fluids when calculating their enhancements. Hence, deviations between experimental and calculated values in Table 3 for the Li data are greater than 3%. In Table 4, large deviations were obtained in fitting the Mursheed[41] and Yoo[109] data because the reported enhancements of 14–18% are unusually high for nanofluids containing 1% (v/v) titania particles. This is also true for the Zhu et al.[42] data for iron oxide nanofluids in Table 8. Zhu et al obtained enhancements of 15–30% in the case of 0.5–1.5% (v/v) iron oxide nanofluids and attributed these high values to alignment of iron oxide nanoparticles. In addition, they also reported a

Table 5. Comparing the Geometric Mean (GM), and Modified Geometric Mean (mGM) Models with Experimental Data for Ceria Nanofluids

				Average Absolute Deviation (%)	
Data Reference	Particle Size (nm)	Fluid	Temperature (K)	GM	mGM (p)
90	12 and 74	Water	298	3.17	2.85 (1)

Table 6. Comparing the Geometric Mean (GM) and Modified Geometric Mean (mGM) Models with Experimental Data for Copper Oxide Nanofluids

				Average Absolute Deviation (%)	
Reference	Particle Size (nm)	Fluid	Temperature (K)	GM	mGM (p)
31	36	Water	298	13.59	14.61 (1)
107	36	Water	298	0.85	0.83 (0.94)
54	23.6	Water	298	6.94	0.99 (0.22)
	23.6	EG	298	3.03	2.37 (0.22)
53	23	Water	298	17.38	2.61 (0.14)
	23	EG	298	32.77	2.37 (0.14)
48	28.6	Water	294–324	8.38	8.99 (1)
113	12	Water	298	0.84	0.4 (1)
55	33	Water	298	0.13	0.58 (1)
	33	EG	298	3.03	3.47 (1)
56	25	Water	298	6.89	6.95 (1)
52	29	Water	302–309	14.59	16.43 (1)
114	29	EG	298	4.47	0.62 (0.37)
32, 33	33	Water	283–303	8.03	0.88 (0.19)

Table 7. Comparing the Geometric Mean (GM) and Modified Geometric Mean (mGM) Models with Experimental Data for Silicon Dioxide Nanofluids

				Average Absolute Deviation (%)	
Reference	Particle Size (nm)	Fluid	Temperature (K)	GM	mGM (p)
55	12	Water	298	2.37	3.52 (1)
13	20	Water	298	1.09	2.82 (1)
111	23	Water	298	1.95	2.55 (1)
	23	EG	298	2.04	2.64 (1)
	23	Ethanol	298	2.32	2.92 (1)

Table 8. Comparing the Geometric Mean (GM) and Modified Geometric Mean (mGM) Models with Experimental Data for Iron Oxide Nanofluids

				Average Absolute Deviation (%)	
Reference	Particle Size (nm)	Fluid	Temperature (K)	GM	mGM (p)
42	10	Water	298	18.82	28.31 (1)

Table 9. Comparing the Geometric Mean (GM) and Modified Geometric Mean (mGM) Models with Experimental Data for Zinc Oxide Nanofluids

				Average Absolute Deviation (%)	
Reference	Particle Size (nm)	Fluid	Temperature (K)	GM	mGM (p)
6	10–60	Water	298	1.77	2.20 (0.32)
	30 and 60	EG	298	2.77	2.93 (0.32)

Table 10. Comparing the Geometric Mean (GM) and Modified Geometric Mean (mGM) Models with Experimental Data for Diamond Nanofluids

				Average Absolute Deviation (%)	
Reference	Particle Size (nm)	Fluid	Temperature (K)	GM	mGM (p)
13	40	EG	298	17.11	18.29 (1)
115	10	Water + EG	298	1.95	14.19 (1)

Table 11. Comparing the Geometric Mean (GM) and Modified Geometric Mean (mGM) Models with Experimental Data for Silicon Carbide Nanofluids

				Average Absolute Deviation (%)	
Reference	Particle Size (nm)	Fluid	Temperature (K)	GM	mGM (p)
116	26 and 900	Water	277	11.51	5.78 (0.03)
	26 and 900	EG	277	13.57	4.31 (0.03)
117	130	Water	296–343	4.27	0.71 (0.13)

nonlinear dependence of thermal conductivity on particle volume fraction for these nanofluids, which is unusual. In the case of diamond nanofluids (Table 10), predictions of the modified geometric mean model appear to be poor because the phonon mean free path for diamond (104.81 nm) is an order of magnitude larger than its particle size (10 nm)[115] It appears that the Liang and Li equation may not be applicable in this case because the equation does not account for quantum size effects.[17] For most nanofluids containing semiconductor or insulator particles, however, the modified geometric mean model provides good estimates of the effective thermal conductivity without any adjustable parameters. If roughness must be accounted for, then one parameter can be included in the model and optimized using data for one base fluid. Thermal conductivities for other base fluids, particle sizes, and temperatures may then be predicted.

Conclusions

This work reviews the effect of key variables on the thermal conductivity of nanofluids and develops a model for the effective thermal conductivity that includes the size-dependence of the thermal conductivity of the particles. The new model, with at most one adjustable parameter, is capable of predicting the effect of different base fluids, particle size, temperature, and volume fraction. Poor model predictions generally imply that experimental values are unusually high or the trends in the data do not conform to expected trends. The model also provides indirect confirmation of the decrease in the thermal conductivity of semiconductor and insulator nanoparticles as the particle size becomes of the same order as the phonon mean free path.

Literature Cited

1. Xuan YM, Li Q. Investigation on convective heat transfer and flow features of nanofluids. *J Heat Trans-Trans ASME*. 2003;125: 151–155.
2. Wen DS, Ding YL. Experimental investigation into the pool boiling heat transfer of aqueous based gamma-alumina nanofluids. *J Nanopart Res*. 2005;7:265–274.
3. Das SK, Choi SUS, Yu W, Pradeep T. *Nanofluids Science and Technology*. New Jersey: Wiley, 2008.
4. Wang XQ, Mujumdar AS. Heat transfer characteristics of nanofluids: a review. *Int J Therm Sci*. 2007;46:1–19.
5. Xie HQ, Wang JC, Xi TG, Liu Y, Ai F, Wu Q. Thermal conductivity enhancement of suspensions containing nanosized alumina particles. *J Appl Phys*. 2002;91:4568–4572.
6. Kim SH, Choi SR, Kim D. Thermal conductivity of metal-oxide nanofluids: particle size dependence and effect of laser irradiation, *J Heat Trans-Trans ASME*. 2007;129:298–307.
7. Keblinski P, Phillpot SR, Choi SUS, Eastman JA. Mechanisms of heat flow in suspensions of nano-sized particles (nanofluids). *Int J Heat Mass Transfer*. 2002;45:855–863.
8. Bird RB, Stewart WE, Lightfoot EN. *Transport Phenomena*, 2nd ed. New York: Wiley, 2002.

9. Meyer CA. editor. *ASME Steam Tables: Thermodynamic and Transport Properties of Steam*, 6th ed. New York: American Society of Mechanical Engineers, 1993.
10. Diguilio R, Teja AS. Thermal conductivity of poly(ethylene glycols) and their binary mixtures. *J Chem Eng Data*. 1990;35:117–121.
11. Doye JPK, Wales DJ. Polytetrahedral clusters. *Phys Rev Lett*. 2001;86:5719–5722.
12. Dean JA. *Lange's Handbook of Chemistry*, 14th ed. New York: McGraw-Hill, 1992.
13. Kang HU, Kim SH, Oh JM. Estimation of thermal conductivity of nanofluid using experimental effective particle volume. *Exp Heat Transfer*. 2006;19:181–191.
14. Choi SUS, Zhang ZG, Yu W, Lockwood FE, Grulke EA. Anomalous thermal conductivity enhancement in nanotube suspensions. *Appl Phys Lett*. 2001;79:2252–2254.
15. Tien C-L, Majumdar A, Gerner FM. editors. *Microscale Energy Transport*. Washington D.C.: Taylor & Francis, 1998.
16. Tien C-L. editor. *Annual Review of Heat Transfer*, Vol. 7. New York: Begell House, 1996.
17. Zhang ZM. *Nano/Microscale Heat Transfer*. Nanoscience and Nanotechnology Series. McGraw Hill Professional, 2007.
18. Ju YS. Phonon heat transport in silicon nanostructures. *Appl Phys Lett*. 2005;87:3.
19. Behkam B, Yang YZ, Asheghi M. Thermal property measurement of thin aluminum oxide layers for giant magnetoresistive (GMR) head applications. *Int J Heat Mass Transfer*. 2005;48: 2023–2031.
20. Liu W, Asheghi M. Phonon-boundary scattering in ultrathin single-crystal silicon layers. *Appl Phys Lett*. 2004;84:3819–3821.
21. Yu XY, Chen G, Verma A, Smith JS. Temperature dependence of thermophysical properties of GAAS/ALAS periodic structure. *Appl Phys Lett*. 1995;67:3554–3556.
22. Cahill DG, Ford WK, Goodson KE, Mahan GD, Majumdar A, Maris HJ, Merlin R, Phillpot SR. Nanoscale thermal transport. *J Appl Phys*. 2003;93:793–818.
23. Ziambaras E, Hyldgaard P. Phonon Knudsen flow in nanostructured semiconductor systems. *J Appl Phys*. 99:054303, 2006.
24. Li DY, Wu YY, Kim P, Shi L, Yang PD, Majumdar A. Thermal conductivity of individual silicon nanowires. *Appl Phys Lett*. 2003;83:2934–2936.
25. Fang KC, Weng CI, Ju SP. An investigation into the structural features and thermal conductivity of silicon nanoparticles using molecular dynamics simulations. *Nanotechnology*. 2006;17:3909–3914.
26. Shin S, Lee SH. Thermal conductivity of suspensions in shear flow fields. *Int J Heat Mass Transfer*. 2000;43:4275–4284.
27. Turian RM, Sung DJ, Hsu FL. Thermal conductivity of granular coals, coal-water mixtures and multi-solid/liquid suspensions. *Fuel*. 1991;70:1157–1172.
28. Choi SUS. Enhancing thermal conductivity of fluids with nanoparticles. In: Siginer DA, Wang HP editors. *Developments and Applications of Non-Newtonian Flows*. New York: AMSE FED-231. 1995:99–105.
29. Eastman JA, Choi SUS, Li S, Yu W, Thompson LJ. Anomalously increased effective thermal conductivities of ethylene glycol-based nanofluids containing copper nanoparticles. *Appl Phys Lett*. 2001; 78:718–720.
30. Jana S, Salehi-Khojin A, Zhong WH. Enhancement of fluid thermal conductivity by the addition of single and hybrid nano-additives. *Thermochim Acta*. 2007;462:45–55.
31. Eastman JA, Choi SUS, Li S, Thompson LJ, Lee S. Enhanced thermal conductivity through the development of nanofluids. *Mater Res Soc Symp Proc (Nanophase and nanocomposite materials II)*. 1997;457:3–11.
32. Zhang X, Gu H., Fujii M Effective thermal conductivity and thermal diffusivity of nanofluids containing spherical and cylindrical nanoparticles. *Exp Therm Fluid Sci*. 2007;31:593–599.
33. Zhang X, Gu H, Fujii M. Experimental study on the effective thermal conductivity and thermal diffusivity of nanofluids. *Int J Thermophys*. 2006;27:569–580.
34. Zhang X, Gu H, Fujii M. Effective thermal conductivity and thermal diffusivity of nanofluids containing spherical and cylindrical nanoparticles. *J Appl Phys*. 2006;100:044325.
35. Timofeeva EV, Gavrilov AN, McCloskey JM, Tolmachev YV, Sprunt S, Lopatina LM, Selinger JV. Thermal conductivity and particle agglomeration in alumina nanofluids: experiment and theory. *Phys Rev E*. 2007;76:061203.
36. Yang Y, Grulke EA, Zhang ZG, Wu GF. Thermal and rheological properties of carbon nanotube-in-oil dispersions. *J Appl Phys*. 2006;99:114307.
37. Beck MP, Yuan Y, Warrier P, Teja AS. The effect of particle size on the thermal conductivity of nanofluids. *J Nanopart Res*. 2009;11:1129–1136.
38. Maxwell JC. *A Treatise on Electricity and Magnetism*, 3rd ed., Vol. II. London: Oxford University Press, 1892.
39. Nan CW, Birringer R, Clarke DR, Gleiter H. Effective thermal conductivity of particulate composites with interfacial thermal resistance. *J Appl Phys*. 1997;81:6692–6699.
40. Yu W, Choi SUS. The role of interfacial layers in the enhanced thermal conductivity of nanofluids: a renovated Maxwell model. *J Nanopart Res*. 2003;5:167–171.
41. Murshed SMS, Leong KC, Yang C. Enhanced thermal conductivity of TiO_2-water based nanofluids. *Int J Therm Sci*. 2005;44:367–373.
42. Zhu HT, Zhang CY, Liu SQ, Tang YM, Yin YS. Effects of nanoparticle clustering and alignment on thermal conductivities of Fe_3O_4 aqueous nanofluids. *Appl Phys Lett*. 2006;89:023123.
43. Liu MS, Lin MCC, Tsai CY, Wang CC. Enhancement of thermal conductivity with Cu for nanofluids using chemical reduction method. *Int J Heat Mass Transfer*. 2006;49:3028–3033.
44. Ceylan A, Jastrzembski K, Shah SI. Enhanced solubility of Ag-Cu nanoparticles and their thermal transport properties. *Metall Mater Trans A*. 2006;37:2033–2038.
45. Putnam SA, Cahill DG, Braun PV, Ge ZB, Shimmin RG. Thermal conductivity of nanoparticle suspensions. *J Appl Phys*. 2006;99:084308.
46. Li CH, Peterson GP. The effect of particle size on the effective thermal conductivity of Al_2O_3-water nanofluids. *J Appl Phys*. 2007;101:044312.
47. Beck MP, Yuan Y, Warrier P, Teja AS. The thermal conductivity of alumina nanofluids in water, ethylene glycol, and ethylene glycol + water mixtures. *J Nanoparticle Res*, in press; DOI 10.1007/s1 1051-009-9716-9.
48. Das SK, Putra N, Thiesen P, Roetzel W. Temperature dependence of thermal conductivity enhancement for nanofluids. *J Heat Trans-Trans ASME*. 2003;125:567–574.
49. Yang B, Han ZH. Temperature-dependent thermal conductivity of nanorod based nanofluids. *Appl Phys Lett*. 2006;89:083111.
50. Beck MP, Sun T, Teja AS. The thermal conductivity of alumina nanoparticles dispersed in ethylene glycol. *Fluid Phase Equilib*. 2007;260:275–278.
51. Xie HQ, Wang JC, Xi TG, Liu Y, Ai F. Dependence of the thermal conductivity of nanoparticle-fluid mixture on the base fluid. *J Mater Sci Lett*. 2002;21:1469–1471.
52. Li CH, Peterson GP. Experimental investigation of temperature and volume fraction variations on the effective thermal conductivity of nanoparticle suspensions (nanofluids). *J Appl Phys*. 2006;99:084314.
53. Wang XW, Xu XF, Choi SUS. Thermal conductivity of nanoparticle-fluid mixture. *J Thermophys Heat Transfer*. 1999;13:474–480.
54. Lee S, Choi SUS, Li S, Eastman JA. Measuring thermal conductivity of fluids containing oxide nanoparticles. *J Heat Trans-Trans ASME*. 1999;121:280–289.
55. Hwang YJ, Ahn YC, Shin HS, Lee CG, Kim GT, Park HS, and Lee JK. Investigation on characteristics of thermal conductivity enhancement of nanofluids. *Curr Appl Phys*. 2006;6:1068–1071.
56. Lee D, Kim JW, Kim BG. A new parameter to control heat transport in nanofluids: surface charge state of the particle in suspension. *J Phys Chem B*. 2006;110:4323–4328.
57. Wright B, Thomas D, Hong H, Groven L, Puszynski J, Duke E, Ye X, Jin S. Magnetic field enhanced thermal conductivity in heat transfer nanofluids containing Ni coated single wall carbon nanotubes. *Appl Phys Lett*. 2007;91:173116.
58. Hong HP, Wright B, Wensel J, Jin SH, Ye XR, Roy W. Enhanced thermal conductivity by the magnetic field in heat transfer nanofluids containing carbon nanotube. *Synth Met*. 2007;157:437–440.

59. Wensel J, Wright B, Thomas D, Douglas W, Mannhalter B, Cross W, Hong HP, Kellar J, Smith P, Roy W. Enhanced thermal conductivity by aggregation in heat transfer nanofluids containing metal oxide nanoparticles and carbon nanotubes. *Appl Phys Lett*. 2008;92:023110.
60. Rayleigh L. On the influence of obstacles arranged in rectangular order upon the properties of a medium. *Philos Mag*. 1892;34:481–502.
61. Hamilton RL, Crosser OK. Thermal conductivity of heterogeneous two-component systems. *Ind Eng Chem Fund*. 1962;1:187–191.
62. Jeffrey DJ. Conduction through a random suspension of spheres. *Proc R Soc London A*. 1973;335:355–367.
63. Progelhof RC, Throne JL, Ruetsch RR. Methods for predicting thermal conductivity of composite systems. *Polym Eng Sci*. 1976;16:615–625.
64. Landauer R. The electrical resistance of binary metallic mixtures. *J Appl Phys*. 1952;23:779–784.
65. Krischer O. *Die Wissenschaftlichen Grundlagen der Trocknungstechnik (The Scientific Fundamentals of Drying Technology)*, 2nd ed. Berlin: Springer-Verlag, 1963.
66. Tsao GTN. Thermal conductivity of 2-phase materials. *Ind Eng Chem*. 1961;53:395–397.
67. Hashin Z, Shtrikman S. A variational approach to the theory of the effective magnetic permeability of multiphase materials. *J Appl Phys*. 1962;33:3125.
68. Nielsen LE. *Predicting the Properties of Mixtures: Mixing Rules in Science and Technology*. New York: Mercer Dekker, 1978.
69. Nan CW. Physics of inhomogeneous inorganic materials. *Prog Mater Sci*. 1993;37:1–117.
70. Prasher R, Evans W, Meakin P, Fish J, Phelan P, Keblinski P. Effect of aggregation on thermal conduction in colloidal nanofluids. *Appl Phys Lett*. 2006;89:143119.
71. Yu W, Choi SUS. The role of interfacial layers in the enhanced thermal conductivity of nanofluids: a renovated Hamilton-Crosser model. *J Nanopart Res*. 2004;6:355–361.
72. Xie HQ, Fujii M, Zhang X. Effect of interfacial nanolayer on the effective thermal conductivity of nanoparticle-fluid mixture. *Int J Heat Mass Transfer*. 2005;48:2926–2932.
73. Xue QZ. Model for thermal conductivity of carbon nanotube based composites. *Physica B*. 2005;368:302–307.
74. Leong KC, Yang C, Murshed SMS. A model for the thermal conductivity of nanofluids - the effect of interfacial layer. *J Nanopart Res*. 2006;8:245–254.
75. Feng YJ, Yu BM, Xu P, Zou MQ. The effective thermal conductivity of nanofluids based on the nanolayer and the aggregation of nanoparticles. *J Phys D: Appl Phys*. 2007;40:3164–3171.
76. Lee D. Thermophysical properties of interfacial layer in nanofluids. *Langmuir*. 2007;23:6011–6018.
77. Li L, Zhang YW, Ma HB, Yang M. An investigation of molecular layering at the liquid-solid interface in nanofluids by molecular dynamics simulation. *Phys Lett A*. 2008;372:4541–4544.
78. Evans W, Fish J, Keblinski P. Thermal conductivity of ordered molecular water. *J Chem Phys*. 2007;126:154504.
79. Jang SP, Choi SUS. Role of Brownian motion in the enhanced thermal conductivity of nanofluids. *Appl Phys Lett*. 2004;84:4316–4318.
80. Koo J, Kleinstreuer C. A new thermal conductivity model for nanofluids. *J Nanopart Res*. 2004;6:577–588.
81. Prasher R, Bhattacharya P, Phelan PE. Thermal conductivity of nanoscale colloidal solutions (nanofluids). *Phys Rev Lett*. 2005;94:025901.
82. Ren Y, Xie H, Cai A. Effective thermal conductivity of nanofluids containing spherical nanoparticles. *J Phys D: Appl Phys*. 2005;38:3958–3961.
83. Xuan YM, Li Q, Zhang X, Fujii M. Stochastic thermal transport of nanoparticle suspensions. *J Appl Phys*. 2006;100:043507.
84. Prakash M, Giannelis EP. Mechanism of heat transport in nanofluids. *J Comput Aided Mater Des*. 2007;14:109–117.
85. Swartz ET, Pohl RO. Thermal boundary resistance. *Rev Mod Phys*. 1989;61:605–668.
86. Prasher R, Evans W, Meakin P, Fish J, Phelan P, Keblinski P. Effect of aggregation on thermal conduction in colloidal nanofluids. *Appl Phys Lett*. 2006;89:143119.
87. Kumar S, Murthy JY. A numerical technique for computing effective thermal conductivity of fluid-particle mixtures. *Numer Heat Transfer Part B*. 2005;47:555–572.
88. Gao L, Zhou XF. Differential effective medium theory for thermal conductivity in nanofluids. *Phys Lett A*. 2006;348:355–360.
89. Chon CH, Kihm KD, Lee SP, Choi SUS. Empirical correlation finding the role of temperature and particle size for nanofluid (Al_2O_3) thermal conductivity enhancement. *Appl Phys Lett*. 2005;87:53107.
90. Beck MP, Yuan Y, Warrier P, Teja AS. Thermal conductivity of aqueous nanofluids containing ceria nanoparticles. *J Applied Phys*, in press.
91. Liang LH, Li B. Size-dependent thermal conductivity of nanoscale semiconducting systems. *Phys Rev B*. 2006;73:153303.
92. Zhang Z, Zhao M, Jiang Q. Melting temperatures of semiconductor nanocrystals in the mesoscopic size range. *Semicond Sci Technol*. 2001;16:L33–L35.
93. Alexander W, Shackelford J. *CRC Materials Science and Engineering Handbook*, 3rd ed. Boca Raton, FL: CRC Press, 2001.
94. NISTwebbook, http://webbook.nist.gov/
95. http://www.ioffe.ru/SVA/NSM/Semicond/
96. Patnaik P. *Handbook of Inorganic Chemicals*. New York: McGraw-Hill, 2002.
97. Hwang Y, Lee JK, Lee CH, Jung YM, Cheong SI, Lee CG, Ku BC, Jang SP, Stability and thermal conductivity characteristics of nanofluids. *Thermochim Acta*. 2007;455:70–74.
98. Slack, G.A. Thermal conductivity of MgO, Al_2O_3, $MgAl_2O_4$, and Fe_3O_4 crystals from 3 degrees to 300 degrees K. *Phys Rev*. 1962;126:427–441.
99. Perry RH, Green DW. editors. *Perry's Chemical Engineers' Handbook*, 7th ed. New York: McGraw-Hill, 1997.
100. Dean JA. *Lange's Handbook of Chemistry*, 14th ed. New York: McGraw-Hill, 1992.
101. Yaws CL. *Chemical Properties Handbook*. New York: McGraw-Hill, 1999.
102. Bragg L, Claringbull GF, Taylor WH. *Crystal Structure of Minerals*. New York: Cornell University Press, 1965.
103. Wen Z, Zhao M, Jiang Q. The melting temperature of molecular nanocrystals at the lower bound of the mesoscopic size range. *J Phys Condens Matter*. 2000;12:8819–8824.
104. Jiang Q, Shi HX, Zhao M. Melting thermodynamics of organic nanocrystals. *J Chem Phys*. 1999;111:2176–2180.
105. Kaviany, M. *Principles of Heat Transfer*, New York: Wiley-Interscience, 2002.
106. Watari K, Nakano H, Sato K, Urabe K, Ishizaki K, Cao S and Mori K. Effect of grain boundaries on thermal conductivity of silicon carbide ceramic at 5 to 1300 K. *J Am Ceram Soc*. 2003; 86:1812–1814.
107. Eastman JA, Choi SUS, Li S, Soyez G, Thompson LJ, DiMelfi RJ. Novel thermal properties of nanostructured materials. *Mater Sci Forum*. 1999;312–314:629–634.
108. Yoo DH, Hong KS, Hong TE, Eastman JA, Yang HS. Thermal conductivity of Al_2O_3/water nanofluids. *J Korean Phys Soc*. 2007;51:S84–S87.
109. Yoo DH, Hong KS, Yang HS. Study of thermal conductivity of nanofluids for the application of heat transfer fluids. *Thermochim Acta*. 2007;455:66–69.
110. Oh DK, Jain A, Eaton JK, Goodson KE, Lee JS. Thermal conductivity measurement and sedimentation detection of aluminum oxide nanofluids by using the 3 omega method. *Int J Heat Fluid Flow*. 2008;29:1456–1461.
111. Wang ZL, Tang DW, Liu S, Zheng XH, Araki N. Thermal-conductivity and thermal-diffusivity measurements of nanofluids by 3 omega method and mechanism analysis of heat transport. *Int J Thermophys*. 2007;28:1255–1268.
112. Wongwises S, Duangthongsuk W. Measurement of temperature-dependent thermal conductivity and viscosity of TiO_2-water nanofluids. *Exp Therm Fluid Sci*. 2009;33:706–714.
113. Kwak K, Kim C. Viscosity and thermal conductivity of copper oxide nanofluid dispersed in ethylene glycol. *Korea-Australia Rheology J*. 2005;17:35–40.
114. Liu MS, Lin MC, Huang IT, Wang CC. Enhancement of thermal conductivity with CuO for nanofluids. *Chem Eng Tech*. 2006;29: 72–77.
115. Xie H, Yu W, Li Y. Thermal performance enhancement in nanofluids containing diamond nanoparticles. *J Phys D: Appl Phys*. 2009;42:095413.

116. Xie HQ, Wang JC, Xi TG, Liu Y, Ai F. Thermal conductivity of suspension containing SiC particles. *J Mater Sci Lett*. 2002;21:193–195.
117. Singh D, Timofeeva W, Yu W, Routbort J, Smith D, Lopez-Cepero JM. An investigation of silicon carbide-water nanofluid for heat transfer applications. *J Appl Phys*. 2009;105:064306.
118. Teja AS, Beck MP, Yuan Y, Warrier P. The limiting behavior of the thermal conductivity of nanoparticles and nanofluids. *J. Appl Phys*., in press; DOI 10.1063/1.3354094.
119. Yang Z, Woo TK, Baudin M, Hermansson K. Atomic and electronic structure of unreduced and reduced CeO_2 surfaces: a first-principles study. *J Chem Phys*. 2004;120:7741–7749.
120. Devanathan R, Gao F, Weber WJ. Atomistic modeling of amorphous silicon carbide using a bond-order potential. *Nucl Instr Meth Phys Res B*. 2007;255:130–135.

Manuscript received July 31, 2009, revision received Oct. 28, 2009, and final revision received Feb. 23, 2010.